

Article

A Study on the Effect of Bond Wires Lift-Off on IGBT Thermal Resistance Measurement

Dan Luo ¹, Minyou Chen ¹, Wei Lai ^{1,*}, Hongjian Xia ¹, Xueni Ding ¹ and Zhenyu Deng ²

¹ State Key Lab of Power Transmission Equipment & System Security and New Technology, School of Electrical Engineering, Chongqing University, Chongqing 400044, China; luodancqu@cqu.edu.cn (D.L.); minyouchen@cqu.edu.cn (M.C.); hongjian_xia@cqu.edu.cn (H.X.); dingxn@cqu.edu.cn (X.D.)

² NXP (Chongqing) Semiconductors Co., Ltd., Chongqing 400044, China; zhenyu.deng@nxp.com

* Correspondence: laiweicqu@cqu.edu.cn

Abstract: Bond wire lift-off will cause an increase of remaining wires' power dissipation, which usually is ignored for healthy modules. However, only partial wires' power dissipation transfers through thermal path from junction to case, which will lead to overestimate the whole power dissipation from collector to emitter pole and underestimate the calculated thermal resistance using the proportion of temperature difference to power dissipation. A FEM model is established to show the change of heat flow after bond wires were removed, the temperature of bond wires increases, and the measured thermal resistance decrease after bond wires lift-off. It is validated by experimental results using open package Insulated Gate Bipolar Transistor (IGBT) modules under different current conditions. This conclusion might be helpful to indicate the bond wires lift-off and solder fatigue by comparing the change of measured thermal resistance. Using the Kelvin setup to measure thermal resistance will cause misjudgment of failure mode due to the ignoring of wires' power dissipation. This paper proposed that the lift-off of bond wires will lead to underestimating the thermal resistance measurement, which will overestimate the lifetime of IGBT module and misjudge its state of health.



Citation: Luo, D.; Chen, M.; Lai, W.; Xia, H.; Ding, X.; Deng, Z. A Study on the Effect of Bond Wires Lift-Off on IGBT Thermal Resistance Measurement. *Electronics* **2021**, *10*, 194. <https://doi.org/10.3390/electronics10020194>

Received: 19 November 2020
Accepted: 12 January 2021
Published: 15 January 2021

Publisher's Note: MDPI stays neutral with regard to jurisdictional claims in published maps and institutional affiliations.



Copyright: © 2021 by the authors. Licensee MDPI, Basel, Switzerland. This article is an open access article distributed under the terms and conditions of the Creative Commons Attribution (CC BY) license (<https://creativecommons.org/licenses/by/4.0/>).

Keywords: IGBT; bond wires lift-off; thermal resistance; heat flow

1. Introduction

Insulated Gate Bipolar Transistors (IGBTs) are widely used in power converter, wind power generation, photovoltaic, aviation, and electric vehicles, hence its reliability has become one of the most important problems in applications [1].

Solder fatigue is one of the domain failure mechanisms in IGBT module [2], a previous study shows the aging of the solder layer causes a rise in junction-to-case thermal resistance [3]. Reference [4] suggested indicates solder fatigue by using a 20% increase in thermal resistance, which are widely used by researchers at present. Hence, thermal resistance is one of the most important indicators to evaluate the reliability of the IGBT module.

Figure 1 shows the structure and material of a wire-bonding IGBT, which consists of several layers of different materials, the thermal resistance of IGBT module consists of IGBT die R_{die} , die-attached solder R_{D-S} , DBC substrate R_{DBC} , baseplate-attached solder R_{B-S} and baseplate R_{base} , as in (1). However, the different sizes and materials of each layer cause a heat spreading angle α between them [5]. This heat spreading angle leads that it is difficult to obtain thermal resistance R_{th} by using (2) [6]. The initial crack and void in the solder surface will also make the calculation of thermal resistance difficult [7].

$$R_{th} = R_{die} + R_{D-S} + R_{DBC} + R_{B-S} + R_{base} \quad (1)$$

$$R \approx \frac{d}{\lambda \times A_{out}} = \frac{d}{\lambda \times (a_{in} + 2 \times d \times \tan \alpha)^2} \quad (2)$$

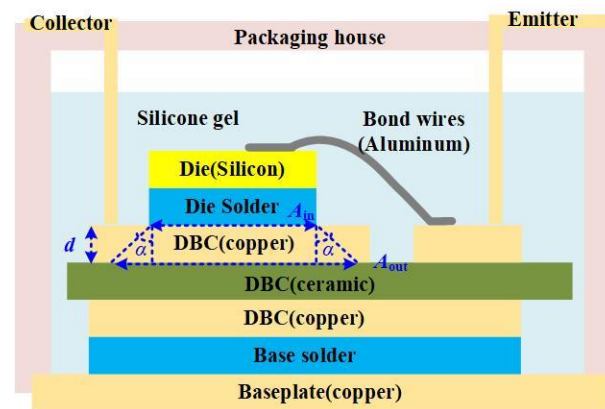


Figure 1. Structure of a wire-bonding Insulated Gate Bipolar Transistors (IGBT) module.

JESD51-1 [8] proposed that the theoretical thermal resistance of semiconductor device R_{th} could be defined by the temperature difference between junction T_J and case T_C divided by power dissipation P in steady-state, as in (3). This method could measure thermal resistance simply and effectively, which is widely used by many researchers.

$$R_{th} = \frac{T_J - T_C}{P} \tag{3}$$

Bond wires lift-off is one of the major failure mechanisms in IGBT module [9], previous researchers had studied a lot of effects of bond wires lift-off on gate voltage [10], conduct voltage [11], or threshold voltage [12]. However, there is still not much study on the effect of lift-off on thermal resistance measurement.

The power dissipation of die is far greater than bond wires, which is less than 3% in healthy module [13]. Therefore, the power dissipation of IGBT module is regarded as die power dissipation in thermal resistance measurement as in Figure 2.

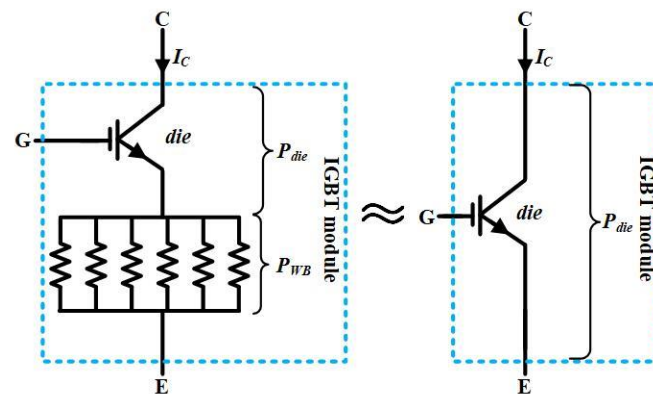


Figure 2. Power dissipation of IGBT module.

Ref. [14] indicated that bond wires lift-off also leads to a rise in junction temperature, which means the power dissipation of wires also affect the thermal resistance calculation.

This paper proposes a study on the effect of bond wires lift-off on thermal resistance measurement. The effect of bond wire lift-off on thermal resistance measurement is presented in Section 2. A FEM model is established in Section 3 to show the change of bond wires' heat flux after lift-off. This conclusion is validated by experimental results under different conditions in Section 4. Test results are discussed in Section 5. Section 6 concludes this paper.

2. Effect of Bond Wires Lift-Off on Thermal Resistance Measurement

The power dissipation of bond wires P_{WB} is far smaller than the die in healthy module [13], hence the die power dissipation P_D is the major heat source in healthy module as in (4).

$$\begin{aligned} P &= P_D + P_{WB} \\ \because P_D &\gg P_{WB} \\ \therefore P &\approx P_D \end{aligned} \tag{4}$$

Usually, the case temperature is measured by the point below the die as in Figure 3. The temperature difference ΔT between junction and case is caused by theoretical thermal resistance and power dissipation in the vertical direction based on (4).

$$\Delta T = T_J - T_C = P_D \times R_{th} \tag{5}$$

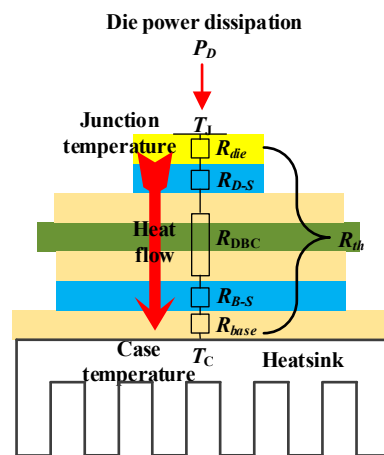


Figure 3. Thermal network in healthy module.

Thus, the measured thermal resistance R_{JC_M} could be extracted based on (3) and (4), which is equal to the theoretical thermal resistance of IGBT module.

$$R_{JC_M} = \frac{T_J - T_C}{P} = \frac{\Delta T}{P_D} = R_{th} \tag{6}$$

Bond wires lift-off leads to a rise in power dissipation of remaining bond wires as in Figure 4a, which means the remaining wires become another heat source. The power dissipation of the remaining wires is shown in (7), where r_{WB_S} is the resistance of a single bond wire, I_C is conduction current, N_{WB} is the number of total bond wires, and N_{fail} is the number of broken wires.

$$P_{WB} = \frac{r_{WB_S}}{N_{WB} - N_{fail}} \times I_C^2 \tag{7}$$

Figure 4b shows that the power dissipation of bond wires transfers to die side P_{WB_D} and emitter side P_{WB_E} , which is different from die's heat flow as in (8).

$$P_{WB} = P_{WB_D} + P_{WB_E} \tag{8}$$

Only P_{WB_D} transfers through the die to the case point in the vertical direction. Hence the power dissipation P' which affects the junction temperature could be obtained as (9).

$$P' = P_D + P_{WB_D} \tag{9}$$

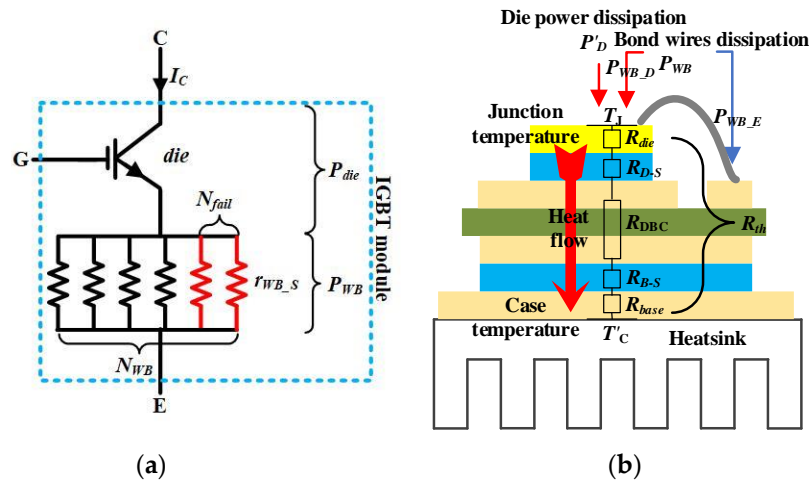


Figure 4. (a) Power dissipation of IGBT module (b) Thermal network after lift-off.

The increased power dissipation leads to a rise in junction temperature after lift-off, as (10). Hence, the theoretical thermal resistance could be obtained as in (11) based on (3), (9) and (10).

$$\Delta T = T_J - T_C = P' \times R_{th} \tag{10}$$

$$R_{th} = \frac{T_J - T_C}{P'} = \frac{\Delta T'}{P_D + P_{WB_D}} \tag{11}$$

Although the rise of junction temperature is caused by P' , the total power dissipation of whole module P_M is measured as the calculated power dissipation in thermal resistance measurement. The relationship between P_M and P' is shown in (12).

$$P_M = P'_D + P_{WB} = (P'_D + P_{WB_D}) + P_{WB_E} = P' + P_{WB_E} \tag{12}$$

Using the module’s power dissipation to measure thermal resistance will lead to a higher calculated power dissipation than the theoretical value. This difference between two power dissipation causes a reduction in measured results R'_{JC-M} after lift-off, which is lower than the theoretical value, as in (13).

$$R'_{JC-M} = \frac{\Delta T'}{P_M} = \frac{P' \times R_{th}}{P_M} = \frac{(P_M - P_{WB_E}) \times R_{th}}{P_M} < R_{th} \tag{13}$$

Bond wires lift-off leads to a rise in power dissipation of remaining wires, while only part of power dissipation transfers through die to case point in the vertical direction. Hence, using the power dissipation of whole module will overestimate the power dissipation and underestimate thermal resistance. Then, this decrement will be more significant with the aging of bond wires.

3. Multiphysic-Modelling Simulation

3.1. Model Building

This paper built a multiphysics field finite-element-method (FEM) model based on a 1200V/50A silicon IGBT module WGL50B120F23 in COMSOL Multiphysics. Two IGBT dies cannot be turned on at the same time due to the half-bridge structure, hence only a single die turns on. The bond wires of diode and gate have been removed to improve computing speed. This FEM model is shown in Figure 5a.

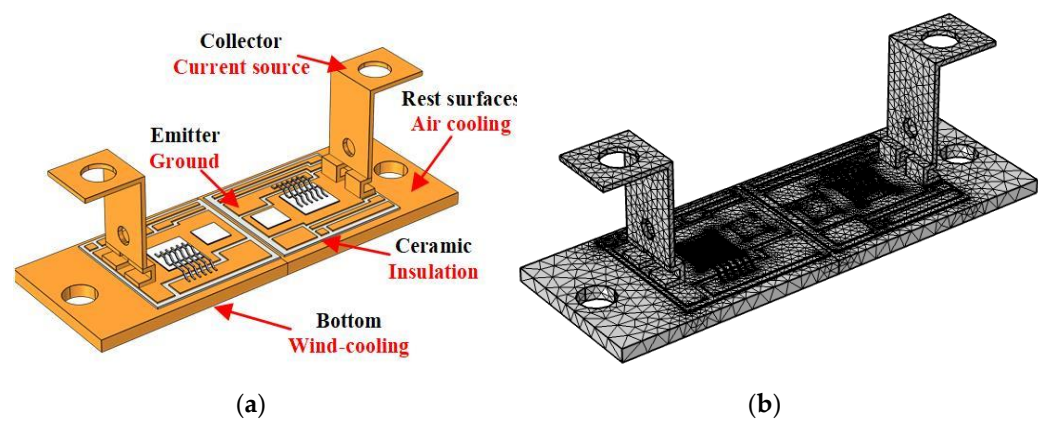


Figure 5. (a) FEM model of IGBT module (b) Meshed FEM model.

Table 1 shows the material properties of FEM model. The electric conductivity of IGBT die is temperature-dependent which can be obtained based on the current-voltage curve [15]. Hence, the pure resistance r_{die} of IGBT die is calculated as in (14), where V_{CE_25} and V_{CE_150} are the conduct voltage at 25 °C and 150 °C at conduct current I . The electrical conductivity of die σ is calculated based on the chip size as in (15), where l , A and T are length, conduct area and temperature of IGBT die, respectively.

$$r_{die} = \frac{V_{CE_25}}{I} + \frac{V_{CE_150} - V_{CE_25}}{I \times (150 - 25)} \times (T - 25) \quad (14)$$

$$\sigma = \frac{1}{r_{die}} \times \frac{l}{A} = \frac{54.52}{(1.5054 + T \times 5.95 \times 10^{-4})} \quad (15)$$

Table 1. Material Properties of FEM Model.

Part	Materials	Density [kg/m ³]	Electric Conductivity [S/m]	Thermal Conductivity [W/(m·K)]
Bond wires	Aluminium	2700	3.5×10^7	237
Die	Silicon	2329	σ	124
Solder	96.5Sn3.5Ag	7400	9.1×10^6	35
Baseplate	Copper	8960	6×10^7	380
Insulation	Al ₂ O ₃	3780	–	30

The ambient temperature sets at 25 °C. The ceramic and all boundaries are set as electric insulation except power supply and ground. A 40A DC source is defined as a terminal with the current source on the collector side and ground potential on the emitter side as electrical boundary conditions in the physical field of Electric Currents Physical Field. A convection coefficient of 3000 W/m²·K is defined on the bottom to simulate as forced air cooling [16] and the rest of the surfaces are defined as 12.5 W/m²·K in the physical field of Heat Transfer in Solids Physical Field. The meshed model is shown in Figure 5b, which consists of 114,813 domain elements, 51,252 boundary elements, and 7059 edge elements. This module is tested with and without bond wires removed.

3.2. Simulation Results

The temperature distributions of IGBT module are shown in Figure 6. The temperature distribution of IGBT module is almost the same after bond wires removed, while the maximum temperature of wires increases from 60.9 °C to 279.9 °C.

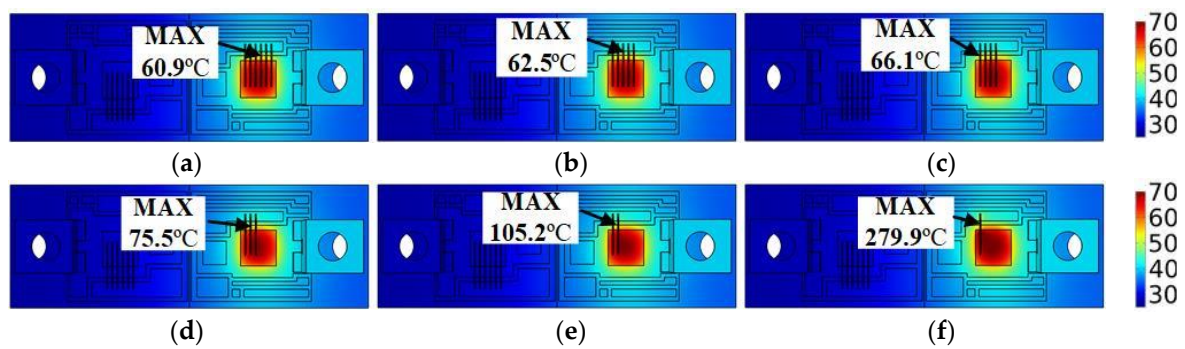


Figure 6. Temperature distribution of IGBT module with different bond wires removed under 40 A (a) 0 wire (b) 1 wire (c) 2 wires (d) 3 wires (e) 4 wires (f) 5 wires.

Figure 7 demonstrates the temperature distribution of die surfaces with different bond wires removed. The average temperature of die is similar after lift-off, where dashed line shows a rise in temperature of bonding area. The highest temperature on die increases from 69.6 °C to 75.2 °C after lift-off, which moved from the centre to bonding area.

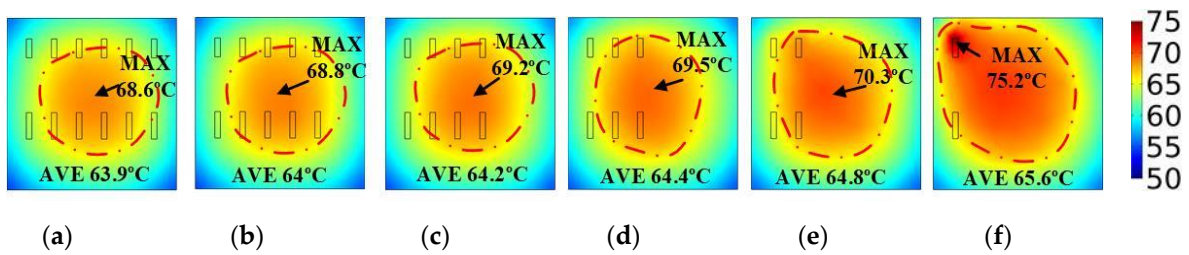


Figure 7. Junction temperature distribution of IGBT die with different wires removed under 40 A (a) 0 wire (b) 1 wire (c) 2 wires (d) 3 wires (e) 4 wires (f) 5 wires.

Figure 8a demonstrates that there is a slowing rise in junction temperature while the temperature of wires increases rapidly after bond wires are removed. The power dissipation of FEM model with different bond wires removed is shown in Figure 8b. The power dissipation of die increases 0.1 W after 5 bond wires removed while power dissipation of bond wires grown six times than before at the same time. The proportion of bond wires power dissipation in IGBT module increase from 1.4% to 8.7% after bond wires removed due to the rise in bond wires' resistance.

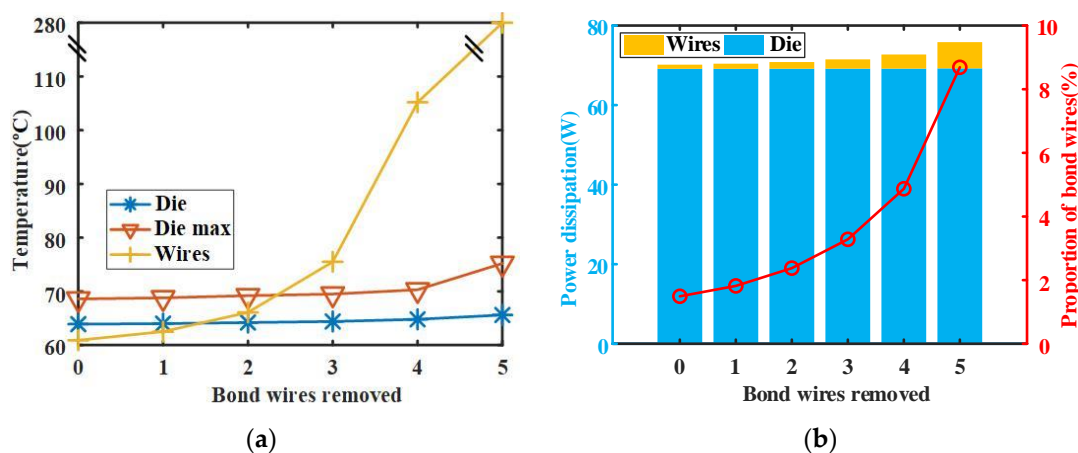


Figure 8. (a) Temperature of die and wires after bond wires removed (b) Power dissipation of die and wires after bond wires removed.

This result shows that power dissipation of IGBT module increase after lift-off, which is mainly caused by the remaining bond wires. This power dissipation of bond wires transfers through die after lift-off and causes a temperature rise.

The cross-sections of simulation results show how bond wires lift-off influence heat flow after bond wires removed, as in Figure 9. The major heat source is die in a healthy module while the heat flow mainly concentrates under chip. The heat flow on emitter side rises a lot after wires removed, which is caused by the heat of wires dissipated through emitter side. Another part of bond wires power dissipation transfer through the die side to the case point. Hence, the die temperature is caused by die power dissipation and part of bond wires power dissipation in the vertical direction.

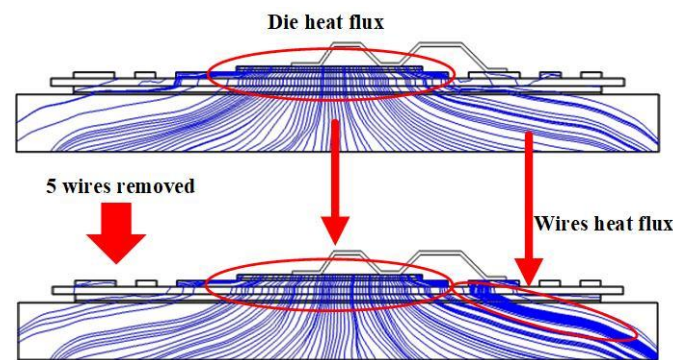


Figure 9. Sectional drawing of the heat flow in IGBT module with and without wires removed.

These simulation results using the power dissipation of whole module are summarized in Table 2. The lift-off of bond wire leads to a rise in power dissipation on remaining wires, which affects junction temperature, wire temperature, and case temperature. However, the measured thermal resistance shows the opposite results. The measured thermal resistance decrement could be calculated as in (16), where R_{JC_0} is the initial calculated thermal resistance before bond wires removed and R_{JC_1} is the calculated thermal resistance after bond wire lift-off. The measured thermal resistance decreases from 0.2591 K/W to 0.2416 K/W after bond wire lift-off, as in Figure 10.

$$\frac{\Delta R_{JC}}{R_{JC}} = \frac{R_{JC_1} - R_{JC_0}}{R_{JC_0}} \times 100\% \quad (16)$$

Table 2. Simulation results.

Wires Removed	0	1	2	3	4	5
T_J (°C)	63.9	64.0	64.2	64.4	64.8	65.6
T_{Jmax} (°C)	68.6	68.8	69.2	69.5	70.3	75.2
T_{wire} (°C)	60.9	62.5	66.1	75.5	105.2	279.9
T_C (°C)	45.65	45.77	45.92	46.02	46.46	47.25
P (W)	70.29	70.53	70.94	71.62	72.84	75.94
R_{JC} (K/W)	0.2591	0.2584	0.2572	0.2565	0.2512	0.2416
$\Delta R_{JC}/R_{JC}$ (%)	0	-0.28	-0.74	-1.01	-3.07	-6.78

These simulation results show that using the power dissipation of the whole module will lead to a decrease in thermal resistance measurement, which will be verified in Section 4.

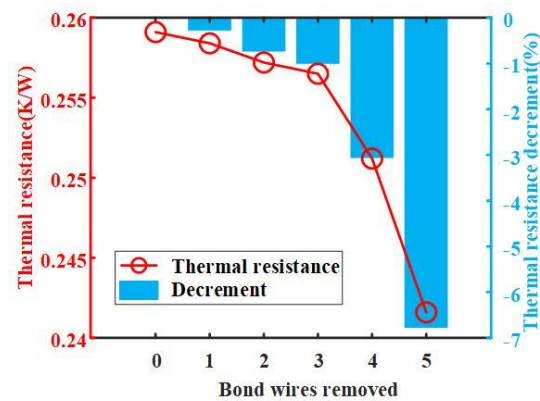


Figure 10. Measured thermal resistance using module's power dissipation.

4. Experimental Results on Bond Wires Lift-Off

4.1. Test Bench

A 1200V/50A IGBT modules from CETC with 6 bond wires on IGBT die 5SMY12H1280 is used in this study. The open package power module free of gel with black-painted is shown in Figure 11a. This module is tested with and without bond wires removal under different current levels. The main electrical circuit for test is shown in Figure 11b. The gate voltage is set at 15 V. A DC power supply is used to test IGBT under different current levels. The collector-emitter voltage is measured by an oscilloscope.

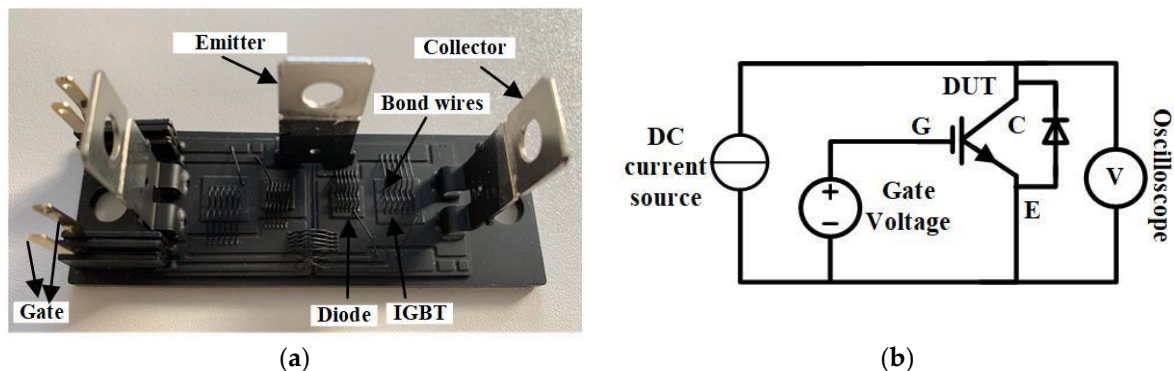


Figure 11. (a) Open package IGBT module, black-painted (b) Main electrical circuit.

A Fan cooled heatsink from GD Rectifiers PS260/xxF is used in this test, as in Figure 12a. Two grooves are incised on the top of the heatsink to place thermal couples, which are used to measure case temperature in a thermocouple data logger (TC08) from PicoLog. A thin thermal pad is attached to the baseplate to reduce air gap between the heatsink and IGBT. The die temperature is measured by an IR camera (Flir A310) above IGBT. This test bench is shown in Figure 12b.

Figure 13a shows that there is a thermal pad between baseplate and heatsink, hence the measured thermal resistance consists of IGBT module R_{JC} thermal pad R_{TP} . There are no other conditions change except bond wires and current levels during detection, the measured thermal resistance R_{JC_M} is equivalent to the junction to case thermal resistance, as in (17).

$$R_{JC_M} = (T_J - T_C) / P = R_{JC} + R_{TP} \quad (17)$$

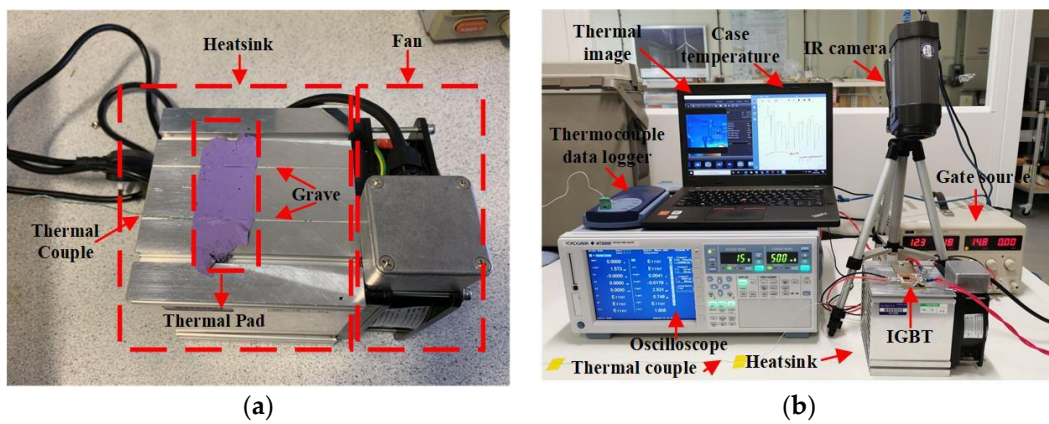


Figure 12. (a) Heatsink (b) Test environment.

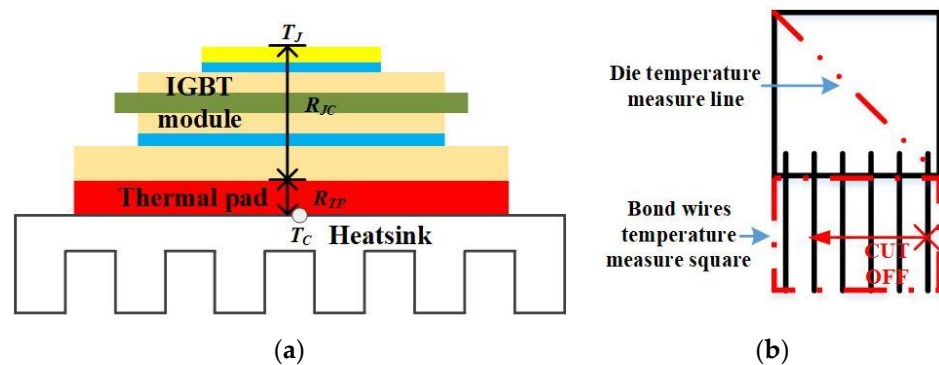


Figure 13. (a) Measured thermal resistance (b) Measured method.

Ref. [14] indicated that it is difficult to detect average die temperature after bond wires lift-off due to the sharp rise of temperature in the bonding area. However, some researchers [17,18] proposed that die temperature could be measured by a line across die after bond wires removed. Hence, this measured method in this paper is shown in Figure 13b, where the temperature of die and the bond wires are measured by mean temperature of line and square. The bond wires are cut from right to left to simulate the aging of bond wires.

4.2. Results Analysis

Figure 14a shows the power dissipation of IGBT module after bond wires removed. The power dissipation increases from 10.87 W to 11.36 W at 10 A after 5 bond wires removed. The power dissipation shows a similar rise at 20 A which is more significant at higher current. The power dissipation increases from 45.3 W to 52.4 W at 30 A with 5 wires removed. Although IGBT bond wire suffers thermal runaway failure at 40 A, it shows a rise of 5 W after 4 bond wires removed.

Figure 14b shows the temperature of die and bond wires under each condition based on Figure 13b, where solid lines are die temperatures and dashed lines are bond wires temperatures. It can be observed that the junction temperature increases slightly while wires temperature rises a lot after bond wires removed. Although bond wire temperature is lower than die at the initial stage, it exceeds die temperature and reaches a higher temperature after bond wires removed.

The slight rise of temperature difference between junction and case indicates that power dissipation increases in the vertical direction, which is caused by an increase of bond wires power dissipation after bond wires removed, as in Figure 14c. The temperature difference stays around 3.6 at 10 A. These results still show a slight rise of 0.2 °C at 20 A.

The rise is more significant at higher current due to higher power dissipation of bond wires, which shows a rise of 1 °C.

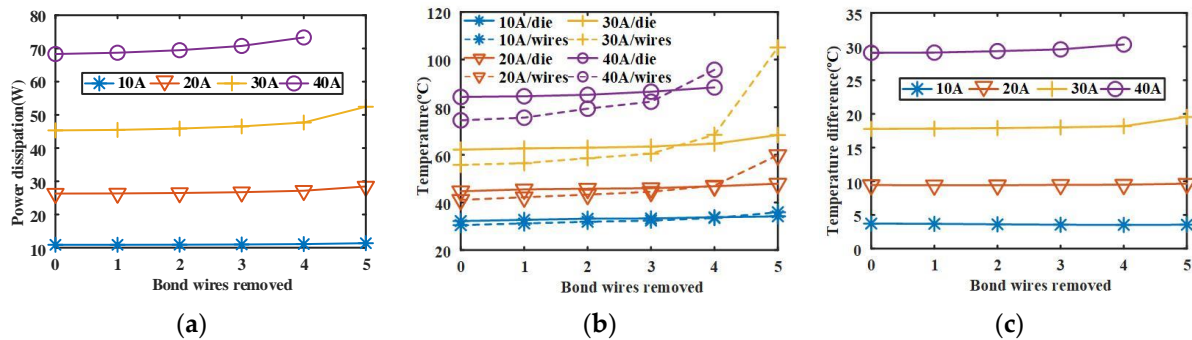


Figure 14. Measured results after bond wires removed (a) Power dissipation of IGBT module (b) Temperature of die and bond wires (c) Temperature difference between die and case.

The power dissipation of bond wires transfers to die side and emitter side, which is affected by the temperatures of two sides. These temperature measuring positions of two sides are shown in Figure 15a. These measured results are shown in Figure 15b, where solid lines are emitter side temperatures and dashed lines are die side temperatures. Although the emitter side temperature increases a bit after bond wires removed, the die side temperature is far higher than the emitter side due to die power dissipation. Hence, most of the heat generated by the bond wires will transfer to emitter side due to its lower temperature according to the second law of thermodynamics.

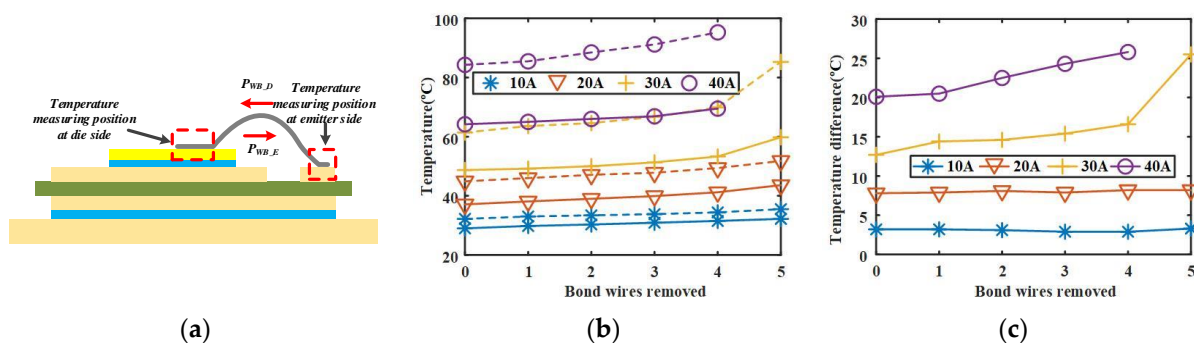


Figure 15. (a) Temperature measuring positions of bond wires two sides (b) Measured temperature of bond wires two sides (c) Temperature difference between two sides of bond wires.

The temperature differences between the two sides of bond wires are shown in Figure 15c. The temperature difference increases slightly at low current after bond wires removed. However, this temperature difference shows a significant rise after bond wires removed under higher current levels, which increase from 12.7 °C to 16.6 °C at 30 A with 5 wires removed as 20.1 °C to 25.8 °C at 40 A with 4 wires removed. The last remaining wire at 30 A even shows a substantial rise of 25.5 °C, which is far higher than initial states.

The uneven temperature distribution on both sides of wires leads extremely difficult to divide the bond wires power dissipation into $P_{WB,E}$ and $P_{WB,D}$, which is not constant for each condition. Hence, it is nearly impossible to calculate the theoretical power dissipation in the vertical direction, which means the measurements of thermal resistance after bond wires lift-off will not be accurate after lift-off.

The operation of the IGBT surface under 30 A with different broken bond wires is demonstrated by IR images in Figure 16, where Ar1 and Li1 are the temperatures of wires and die. Initially, the junction temperature is higher than bond wires temperature, as in Figure 16a,b. The wires get hotter and show higher maximum temperature than die after

several wires removed, as in Figure 16c,d. Finally, the average temperature of bond wires is higher than die with far greater maximum temperature, as in Figure 16e,f.

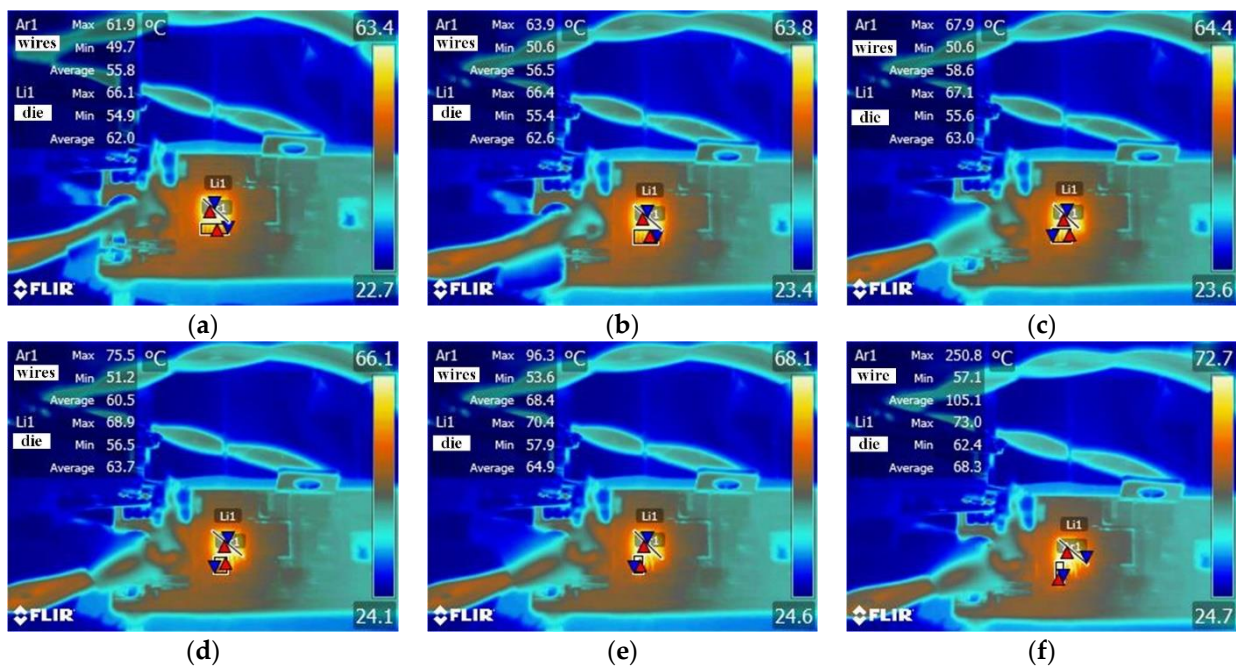


Figure 16. Thermal images of an IGBT device under 30 A with different wires removed (a) 0 wire (b) 1 wire (c) 2 wires (d) 3 wires (e) 4 wires (f) 5 wires.

The measured junction-to-case thermal resistance after bond wires removed is shown in Figure 17, where solid lines are measured thermal resistance and dashed lines are decrement. The first two bond wires removed show a small effect on thermal resistance measurement due to the small power dissipation increase at the initial stage. Then, the thermal resistance decrement is 1.3% with three bond wires removed. Compared with the initial value, the thermal resistance decreases to 2.8% with four bond wires removed, which finally reaches 5% with only one remaining wire. Although the initial measured thermal resistances are different for each current level, they all show a similar decreasing trend after bond wires removed. The obtained values are summarized in Table 3.

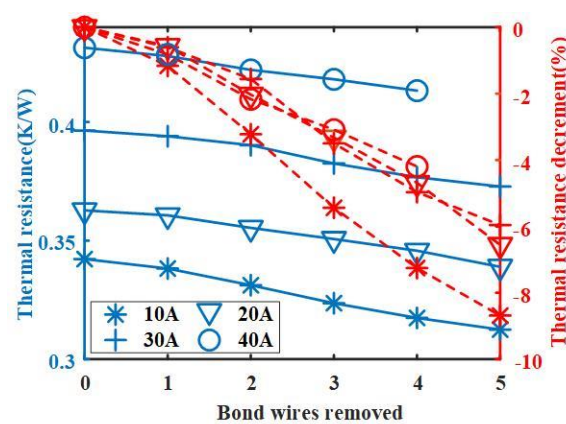


Figure 17. Measured thermal resistance after bond wires lift-off.

Table 3. Thermal resistance (K/W) under different working conditions after bond wires removed.

Current	0 Wire Fail	1 Wire Fail	2 Wires Fail	3 Wires Fail	4 Wires Fail	5 Wires Fail
10 A	0.3422	0.3382	0.3312	0.3236	0.3174	0.3125
	0.00%	-1.17%	-3.22%	-5.44%	-7.25%	-8.69%
20 A	0.3589	0.3569	0.3554	0.3544	0.3494	0.3390
	0.00%	-0.57%	-1.00%	-1.26%	-2.65%	-5.57%
30 A	0.3920	0.3918	0.3902	0.3868	0.3809	0.3728
	0.00%	-0.05%	-0.45%	-1.32%	-2.83%	-4.90%
40 A	0.4255	0.4235	0.4220	0.4180	0.4133	–
	0.00%	-0.48%	-0.82%	-1.75%	-2.88%	–

5. Discussion

5.1. Factors affecting Thermal Resistance Measurement

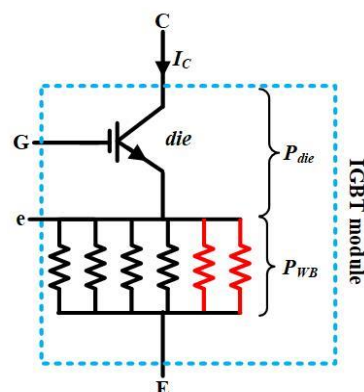
JESD51-1 proposes to measure an accurate measurement of thermal resistance with at least 20 °C temperature rise on die. The measured results are more accurate at higher current due to the larger temperature rise on die. However, the temperature rise is far less than 20 °C at low current level due to small power dissipation, which also makes it difficult to detect the change of case temperature.

The test results show similar results at higher current while thermal resistance decrement is more significant at 10 A, which is caused by inaccuracy junction temperature measurement at small current. The open package structure might lead to heat spreading for all dimensions [19] and cause a change in thermal resistance measured. These reasons finally cause different initial thermal resistance.

This paper shows that only part of bond wires' power dissipation transfers to die side after bond wires lift-off. Hence some temperature sensitivity detection methods, which use whole module's conduct voltage [20] or gate voltage [17], will get a higher result after bond wires lift-off. Those methods which propose to use dynamic time characteristics to measure junction temperatures, such as turn-on delay [21] and turn-off delay [22], could provide accurate results after bond wire lift-off.

5.2. Using Die Power Dissipation to Measure Thermal Resistance

Although Figure 18 shows that the Kelvin setup could measure the die power dissipation from Collector terminal *C* and Auxiliary emitter terminal *e*, it still leads to a confusing result in thermal resistance measurement.

**Figure 18.** Power dissipation of IGBT module using Kelvin setup.

The die power dissipation is smaller than the theoretical power dissipation in the vertical direction, which ignored the effect of P_{WB_D} on junction temperature. Thus, using

the die power dissipation as the calculated power dissipation will lead to a rise in measured thermal resistance R''_{JC-M} as in (18).

$$R''_{JC-M} = \frac{\Delta T'}{P_D} = \frac{P' \times R_{th}}{P_d} = \frac{(P_D + P_{WB,D}) \times R_{th}}{P_D} > R_{th} \quad (18)$$

The measured thermal resistance of FEM model by using die power dissipation is shown in Figure 19. The measured thermal resistance increases after bond wires removed, which shows similar performance as solder fatigue. These results are caused by ignoring of wires' power dissipation. Hence, using the Kelvin setup to measure thermal resistance will cause misjudgment of failure mode.

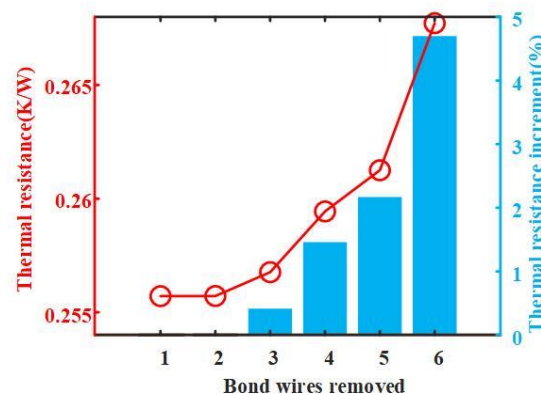


Figure 19. Measured thermal resistance using die power dissipation.

5.3. Failure Criteria Based on Thermal Resistance Decrement

Ref. [23] proposed to use a 5% rise in conduct voltage as the failure criteria of bond wires, which are widely used by lots of researchers [14,24,25] to indicate the failure of bond wires. However, it is still very difficult to distinguish the failure of bond wires due to the similar performance as solder fatigue. However, this feature of decrement in thermal resistance measurement might be useful in fault detection.

The measured thermal resistances at failure critical under each current level are shown in Table 4. The difference between decrement of each current condition is caused by the remaining wires at failure criteria, which shows 1 wire remains at lower current and 2 wires remain at higher current.

Table 4. Failure Criteria of Bond Wires Lift-Off.

Conduct Current	Initial Voltage	5% Voltage Increase	Failure Voltage	Wires Remain	Thermal Resistance Decrement
10 A	1.087	1.1414	1.136	1	-8.69%
20 A	1.315	1.3808	1.422	1	-5.57%
30 A	1.511	1.5866	1.59	2	-2.83%
40 A	1.708	1.7934	1.833	2	-2.88%

Although the test results show that the decrement at the failure point is different for each current level, they show the opposite results of solder fatigue. The solder fatigue of IGBT modules increases die power dissipation [26], which also leads to a rise in the module's power dissipation. However, the calculated thermal resistance increases after solder fatigue, which is different from bond wires lift-off, as in Figure 20. These different effects of two aging processes on thermal resistance measurement might be helpful to indicate the failure of IGBT bond wires lift-off and solder fatigue by using the rising and falling of measured results.

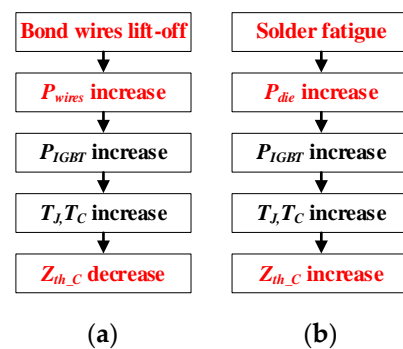


Figure 20. Effect of failure mechanism on thermal resistance measurement (a) bond wires lift-off (b) solder fatigue.

6. Conclusions

This paper proposes a study on the effect of bond wire lift-off on thermal resistance measurement. The analysis leads to following conclusions:

(1) Bond wire lift-off leads to a rise in power dissipation of remaining bond wires, and the power dissipation transfers through the die side and emitter side respectively. However, only part of the power dissipation passing through the die will cause the junction temperature to rise. Hence, the thermal resistance will be underestimated because the power dissipation is overestimated when using the power dissipation of whole module to calculate the thermal resistance.

(2) In the tests, the thermal resistance is measured under different current conditions with and without bond wires removed. Measured results are compared with the initial value, which all show a decrease after bond wires removed. Reference [3] indicated that even a 0.5% increase of thermal resistance could lead to a significant impact on lifetime estimation. This paper proposed that the lift-off of bond wires will lead to underestimating the thermal resistance measurement, which will overestimate the lifetime of IGBT module and misjudge its state of health. Thus, the effect of bond wires lift-off on thermal resistance measurement needs to be taken seriously to improve the reliability of IGBT module.

(3) This paper proposed that the decrement of thermal resistance calculated is caused by bond wires lift-off, which is opposite to solder fatigue. Hence, the changes in thermal resistance measurement might be helpful to distinguish fatigue of IGBT module under different conditions. In future work, the detection method of bond wires fatigue based on thermal resistance decrement will be further studied to avoid the open-circuit fault of IGBT module.

Author Contributions: Conceptualization, methodology, validation and writing—original draft preparation, D.L.; writing, review and editing, W.L., H.X., X.D. and Z.D.; supervision, W.L. and M.C. All authors have read and agreed to the published version of the manuscript.

Funding: This research was supported by the National Key Research and Development Program of China (grant numbers 2018YFB0905800); the National Natural Science Foundation of China (grant numbers 51707024); the Fundamental Research Funds for the Central Universities Project (No.2020CDJQY-A026) and the National “111” Project (B08036).

Data Availability Statement: The data presented in this study are available on request from the corresponding author.

Acknowledgments: The authors would like to thank Li Ran, Ruizhu Wu, Borong Hu, and Xuan Guo at the University of Warwick for the help and advice.

Conflicts of Interest: The authors declare no conflict of interest.

References

1. Yang, S.; Bryant, A.; Mawby, P.; Xiang, D.; Ran, L.; Tavner, P. An Industry-Based Survey of Reliability in Power Electronic Converters. *IEEE Trans. Ind. Appl.* **2011**, *47*, 1441–1451. [[CrossRef](#)]
2. Lai, W.; Chen, M.; Ran, L.; Xu, S.; Jiang, N.; Wang, X.; Alatise, O.; Mawby, P. Experimental Investigation on the Effects of Narrow Junction Temperature Cycles on Die-Attach Solder Layer in an IGBT Module. *IEEE Trans. Power Electron.* **2017**, *32*, 1431–1441. [[CrossRef](#)]
3. Lai, W.; Chen, M.; Ran, L.; Alatise, O.; Xu, S.; Mawby, P. Low Stress Cycle Effect in IGBT Power Module Die-Attach Lifetime Modeling. *IEEE Trans. Power Electron.* **2016**, *31*, 6575–6585. [[CrossRef](#)]
4. Scheuermann, U. Reliability of pressure contacted intelligent integrated power modules. In Proceedings of the 14th International Symposium on Power Semiconductor Devices and Ics, Nuremberg, Germany, 7 June 2002; pp. 249–252. [[CrossRef](#)]
5. Lostetter, A.; Barlow, F.; Elshabini, A. An overview to integrated power module design for high power electronics packaging. *Microelectron. Reliab.* **2000**, *40*, 365–379. [[CrossRef](#)]
6. Wang, Z.; Qiao, W.; Qu, L. A Real-Time Adaptive IGBT Thermal Model Based on an Effective Heat Propagation Path Concept. *IEEE J. Emerg. Sel. Top. Power Electron.* **2020**, *1*. [[CrossRef](#)]
7. Li, J.; Yaqub, I.; Corfield, M.; Johnson, C.M. Interconnect Materials Enabling IGBT Modules to Achieve Stable Short-Circuit Failure Behavior. *IEEE Trans. Compon. Packag. Manuf. Technol.* **2017**, *7*, 734–744. [[CrossRef](#)]
8. INTEGRATED CIRCUIT THERMAL MEASUREMENT METHOD—ELECTRICAL TEST METHOD. Available online: <https://www.jedec.org/standards-documents/docs/jesd-51-1> (accessed on 1 December 1995).
9. Baker, N.; Liserre, M.; Dupont, L.; Avenas, Y. Improved Reliability of Power Modules: A Review of Online Junction Temperature Measurement Methods. *IEEE Ind. Electron. Mag.* **2014**, *8*, 17–27. [[CrossRef](#)]
10. Zhou, L.; Zhou, S.; Xu, M. Investigation of gate voltage oscillations in an IGBT module after partial bond wires lift-off. *Microelectron. Reliab.* **2013**, *53*, 282–287. [[CrossRef](#)]
11. Smet, V.; Forest, F.; Huselstein, J.-J.; Rashed, A.; Richardeau, F. Evaluation of Vce Monitoring as a Real-Time Method to Estimate Aging of Bond Wire-IGBT Modules Stressed by Power Cycling. *IEEE Trans. Ind. Electron.* **2012**, *60*, 2760–2770. [[CrossRef](#)]
12. Mandeya, R.; Chen, C.; Pickert, V.; Naayagi, R.; Ji, B. Gate-Emitter Pre-threshold Voltage as a Health-Sensitive Parameter for IGBT Chip Failure Monitoring in High-Voltage Multichip IGBT Power Modules. *IEEE Trans. Power Electron.* **2018**, *34*, 9158–9169. [[CrossRef](#)]
13. Choi, U.; Blaabjerg, F. Separation of Wear-Out Failure Modes of IGBT Modules in Grid-Connected Inverter Systems. *IEEE Trans. Power Electron.* **2017**, *33*, 6217–6223. [[CrossRef](#)]
14. Ji, B.; Pickert, V.; Cao, W.; Zahawi, B. In Situ Diagnostics and Prognostics of Wire Bonding Faults in IGBT Modules for Electric Vehicle Drives. *IEEE Trans. Power Electron.* **2013**, *28*, 5568–5577. [[CrossRef](#)]
15. Gao, B.; Yang, F.; Chen, M.; Ran, L.; Ullah, I.; Xu, S.; Mawby, P. A Temperature Gradient-Based Potential Defects Identification Method for IGBT Module. *IEEE Trans. Power Electron.* **2017**, *32*, 2227–2242. [[CrossRef](#)]
16. Bahman, A.S.; Ma, K.; Blaabjerg, F. A Lumped Thermal Model Including Thermal Coupling and Thermal Boundary Conditions for High-Power IGBT Modules. *IEEE Trans. Power Electron.* **2018**, *33*, 2518–2530. [[CrossRef](#)]
17. Baker, N.; Dupont, L.; Munk-Nielsen, S.; Iannuzzo, F.; Liserre, M. IR Camera Validation of IGBT Junction Temperature Measurement via Peak Gate Current. *IEEE Trans. Power Electron.* **2017**, *32*, 3099–3111. [[CrossRef](#)]
18. Dupont, L.; Avenas, Y.; Jeannin, P.-O. Comparison of Junction Temperature Evaluations in a Power IGBT Module Using an IR Camera and Three Thermosensitive Electrical Parameters. *IEEE Trans. Ind. Appl.* **2013**, *49*, 1599–1608. [[CrossRef](#)]
19. Schweitzer, D.; Pape, H.; Chen, L. Transient Measurement of the Junction-To-Case Thermal Resistance Using Structure Functions: Chances and Limits. In Proceedings of the Twenty-Third Annual IEEE Semiconductor Thermal Measurement and Management Symposium, San Jose, CA, USA, 16–20 March 2008; pp. 191–197.
20. Perpina, X.; Serviere, J.; Saiz, J.; Barlini, D.; Mermet-Guyennet, M.; Millán, J. Temperature measurement on series resistance and devices in power packs based on on-state voltage drop monitoring at high current. *Microelectron. Reliab.* **2006**, *46*, 1834–1839. [[CrossRef](#)]
21. Harald, K.; Axel, M. On-line junction temperature measurement of IGBTs based on temperature sensitive electrical parameters. In Proceedings of the 2009 13th European Conference on Power Electronics and Applications, Barcelona, Spain, 8–10 September 2009; pp. 2249–2258.
22. Luo, H.; Chen, Y.; Sun, P.; Li, W.; He, X. Junction Temperature Extraction Approach with Turn-off Delay Time for High-voltage High-Power IGBT Modules. *IEEE Trans. Power Electron.* **2015**, *31*, 1. [[CrossRef](#)]
23. Held, M.; Jacob, P.; Nicoletti, G.; Scacco, P.; Poech, M.-H. Fast power cycling test of IGBT modules in traction application. In Proceedings of the Second International Conference on Power Electronics and Drive Systems, Singapore, 26–29 May 1997; pp. 425–430.
24. Andreas, B. A Novel Test Method for Minimising Energy Costs in IGBT Power Cycling Studies. Ph.D Thesis, University of the Witwatersrand, Johannesburg, South African, 2006.
25. Wei, K.; Du, M.; Xie, L.; Li, J. Study of Bonding Wire Failure Effects on External Measurable Signals of IGBT Module. *IEEE Trans. Device Mater. Reliab.* **2012**, *14*, 83–89. [[CrossRef](#)]
26. Lai, W.; Chen, M.; Ran, L.; Xu, S.; Qin, H.; Alatise, O.; Mawby, P.A. Study on the lifetime characteristics of power modules under power cycling conditions. *IET Power Electron.* **2016**, *9*, 1045–1052. [[CrossRef](#)]